mRNA expression and DNA methylation analysis of the inhibitory mechanism of H_2O_2 on the proliferation of A549 cells

YEPENG LI[1], ZHONGHENG WEI[1], SHIQING HUANG[1] and BO YANG[2]

[1]Department of Oncology, [2]Key Laboratory of Guangxi College and Universities, Biomedical Research Center, The Affiliated Hospital of Youjiang Medical University for Nationalities, Baise, Guangxi Zhuang Autonomous Region 533000, P.R. China

Received October 31, 2019; Accepted August 18, 2020

DOI: 10.3892/ol.2020.12151

Abstract. Reactive oxygen species, particularly hydrogen peroxide (H_2O_2), can induce proliferation inhibition and death of A549 cells via oxidative stress. Oxidative stress has effect on DNA methylation. Oxidative stress and DNA methylation feature a common denominator: The one carbon cycle. To explore the inhibitory mechanism of H_2O_2 on the proliferation of lung cancer cells, the present study analysed the mRNA expression and methylation profiles in A549 cells treated with H_2O_2 for 24 h, as adenocarcinoma is the most common pathological type of lung cancer. The DNA methylation profile was constructed using reduced representation bisulphite sequencing, which identified 29,755 differentially methylated sites (15,365 upregulated and 14,390 downregulated), and 1,575 differentially methylated regions located in the gene promoters were identified using the methylKit. Analysis of the assocaition between gene expression and methylation levels revealed that several genes were downregulated and hypermethylated, including cyclin-dependent kinase inhibitor 3, denticleless E3 ubiquitin protein ligase homolog, centromere protein (CENP)F, kinesin family member (KIF)20A, CENPA, KIF11, PCNA clamp-associated factor and GINS complex subunit 2, which may be involved in the inhibitory process of H_2O_2 on the proliferation of A549 cells.

Introduction

Reactive oxygen species (ROS), whose principal components include superoxide anion (O_2^-), hydrogen peroxide (H_2O_2) and hydroxyl radical, can be generated in all aerobic cells (1). At normal concentrations, ROS can be regarded as signalling molecules, whereas high concentrations of ROS are cytotoxic, often leading to cell death (2). Lung cancer is one of the most malignant tumours in the respiratory tract, and 85% of lung cancer cases are non-small cell lung cancer (NSCLC) (3). Previous reports have revealed that H_2O_2 may inhibit the proliferation of A549 lung cancer cells via oxidative stress (4,5). A recent study demonstrated that in lung cancer cells treated with H_2O_2, MAPK inhibitors (mainly the JNK inhibitor) increased O_2^- and glutathione depletion, thus leading to cell death (6). Furthermore, oligomeric proanthocyanidins have been reported to protect A549 cells from oxidative stress induced by H_2O_2 through the Nrf2-antioxidant responsive element signalling pathway (7).

DNA methylation is a biochemical process that occurs with the addition of methyl groups to cytosines adjacent to guanines (CpG) by DNA methyltransferases (8). Although DNA methylation is mainly located in the gene promoter region, it can also occur along the gene sequence, and different locations correspond to different effects on the gene expression level (9,10). DNA methylation can regulate gene expression, as well as maintain the DNA structure and control the transposable elements; therefore, it is often associated with various processes, such as tissue differentiation and disease susceptibility (11,12). Anglim *et al* (13) identified several useful DNA methylation markers for the early detection of squamous cell lung cancer using DNA methylation profiles. Del Real *et al* (14) identified two long non-coding RNAs that may promote the pathological process of non-small cell lung cancer by analysing gene expression and methylation profiles.

In the present study, genome-wide analyses of mRNA expression and DNA methylation were systematically performed to evaluate the inhibitory mechanism of H_2O_2 on the proliferation of A549 cells. Association analysis of differentially expressed genes (DEGs) and differentially methylated regions (DMRs) revealed several genes that may be associated with the inhibitory process of H_2O_2 on the proliferation of A549 cells. The present study may provide novel insights into the molecular mechanisms underlying the inhibitory effects of H_2O_2 on the proliferation of A549 cells, and could contribute to the identification of novel prognostic or diagnostic markers for lung cancer.

Materials and methods

Cell culture. A549 lung cancer cells were purchased from the Cell Bank of Type Culture Collection of the Chinese Academy

Correspondence to: Dr Bo Yang, Key Laboratory of Guangxi College and Universities, Biomedical Research Center, The Affiliated Hospital of Youjiang Medical University for Nationalities, 18 Zhongshan Second Road, Baise, Guangxi Zhuang Autonomous Region 533000, P.R. China
E-mail: yangbo1977@hotmail.com

Key words: mRNA expression, DNA methylation, H_2O_2, A549 cells

of Sciences. A549 cells were cultured in RPMI-1640 medium containing 10% FBS (Ausbian, http://www.viansaga.com/ausbian.html), 2 mM L-glutamine, 100 U/ml penicillin and 100 mg/ml streptomycin at 37˚C in a 5% CO_2 incubator. Cells treated only with culture medium were used as the control group, whereas cells treated with H_2O_2 for 24 h at 37˚C with a final concentration of 200 μM constituted the experimental group. The original images of H_2O_2-treated and untreated A549 cells were captured using a light microscope. After counting, the cells in both groups were inoculated on corresponding culture plates for further analysis, with ~10^6 cells used for the gene expression microarray and reduced representation bisulphite sequencing (RRBS).

MTT assay. Cell viability was assessed using the MTT assay. A549 cells were seeded at a density of 4,000 cells/well in a 96-well plate and incubated with H_2O_2 at 37˚C for 24 h. Subsequently, 20 μl MTT aqueous solution (5 mg/ml) was added to each well and the plates were incubated for 4 h at 37˚C in a humidified atmosphere containing 5% CO_2. The culture medium was aspirated and 100 μl DMSO was added to each well. Finally, ELX800 UV universal microplate reader (Bio-Tek Instruments Inc.) was used to determine the absorbance at 570 nm with a reference wavelength of 630 nm.

Half maximal inhibitory concentration (IC_{50}) calculation. The IC_{50} value, which is the concentration that inhibited cell viability to 50% of the control, was used to evaluate the inhibitory effect of H_2O_2 on the proliferation of A549 cells. GraphPad Prism (version 5; GraphPad Software, Inc.) was used to calculate the IC_{50} value from the best-fit of the Hill slope curve using nonlinear regression analysis: M = 100/1 + 10^[($LogIC_{50}$-N) x HillSlope)], where N is the log of the dose, M is the growth inhibition value normalised to the control and HillSlope is the unitless slope factor or Hill slope.

ROS assay. The Fluorometric Intracellular ROS Assay kit (Sigma-Aldrich; Merck KGaA) was used to detect ROS produced by H_2O_2-treated A549 cells, according to the manufacturer's protocol. The assay was performed in 96-well plate and read using a fluorescence microplate reader resulting in a fluorometric product (l ex = 490/l em = 520 nm) proportional to the amount of ROS present.

Identification of DEGs and RRBS assay. The treated cells were collected by centrifugation at 8,000 x g at 4˚C for 1 min separately, the DNA was extracted using the cetyltrimethylammonium bromide method according to the DNA extract kit manufacurer's protocol (Roche Diagnostics) and the RNA was extracted using TRIzol® (Invitrogen; Thermo Fisher Scientific, Inc.), according to the operating instructions.

RRBS assay. After genomic DNA was extracted from the samples, DNA concentration and integrity were detected using a NanoDrop spectrophotometer (NanoDrop; Thermo Fisher Scientific, Inc.) and 1% agarose gel electrophoresis, respectively. The DNA libraries for bisulphite sequencing were prepared as previously described (15). Briefly, genomic DNA was fragmented into 100-300 bp via sonication with a duration 30 sec at 30 sec intervals for 15 cycles at 20 kHz and 4˚C (Covaris M220) and purified using the MiniElute PCR Purification kit (Qiagen, Inc.). The DNA fragments were end-repaired and a single 'A' nucleotide was added to the 3'-end of the blunt fragments. Subsequently, the genomic fragments were ligated to methylated sequencing adapters. Fragments with adapters were bisulphite-converted using the Methylation-Gold kit (Zymo Research Corp.). Finally, the converted DNA fragments were amplified via PCR and sequenced using Illumina HiSeq™ 2500 by Shanghai GeneChem Co., Ltd.

Table I. Primers used for reverse transcription-quantitative PCR.

Primer name	Sequence (5'→3')
(h)CDKN3-138-F	ACAGAAGGACGAACCAGTGAG
(h)CDKN3-138-R	TTGTATTGAACTGGGCGGCT
(h)CENPF-99-F	CGTCCCCGAGAGCAAGTTTAT
(h)CENPF-99-R	TGTAGGCAGCCCTTCTTTCC
(h)HIST1H2BM-151-F	CGACCATCACTTCGAGGGAG
(h)HIST1H2BM-151-R	GTCACGGCGGAACTGTTACT
GAPDH-127-F (h)	CCAGGTGGTCTCCTCTGA
GAPDH-127-R (h)	GCTGTAGCCAAATCGTTGT

F, forward; R, reverse; h, human; CDKN3, cyclin-dependent kinase inhibitor 3; CENPF, centromere protein F; HIST1H2BM, histone cluster 1 H2B family member M.

Identification of DEGs: Genome-wide expression profiling analysis was performed by Genminix Informatics Co., Ltd. using GeneChip ClarionD Array (Affymetrix; Thermo Fisher Scientific, Inc.). Briefly, total RNA was separately extracted from 10 individual samples using the RNeasy Mini kit (Qiagen, Inc.). Double-stranded cDNA was then synthesized, labeled and hybridized to the gene chip. After hybridization and washing, the slides were scanned with the GeneChip Operating Software version 4.0 (Affymetrix; Thermo Fisher Scientific, Inc.). Raw data extraction and subsequent data processing were performed using the Affymetrix GeneChip Operating Software.

The significant differential analysis was conducted via unpaired Student's t-tests to identify the DEGs between H_2O_2-treated A549 cells and the control group. Only genes that met the cut-off criteria (adjusted $P<0.05$ and $|Fold\ Change| >2$) were regarded as significantly differentially expressed. Additionally, the DEGs were clustered using the hierarchical clustering method and Euclidean distance was chosen as a measure of the distance between the samples. The clustering was implemented using the heatmap.2 function in the gplot R package version 3.6.3 (https://www.rdocumentation.org/packages/gplots/).

Quantitative gene expression analysis via reverse transcription-quantitative (RT-q)PCR. RT-qPCR assays were performed to validate the microarray data. Total RNA was extracted from A549 cells using TRIzol reagent. Single-strand cDNA was synthesized from 1 mg total RNA using the Prime-Script™ Reagent kit with gDNA Eraser (TransGen Biotech Co., Ltd.). The steps were 70˚C for 5 min, 37˚C for 5 min, 42˚C for 60 min and 70˚C for 10 min to end the reaction. To detect the mRNA expression levels of the DEGs, qPCR (TaqMan kit; Thermo Fisher Scientific, Inc.) was conducted on a Q1 PCR

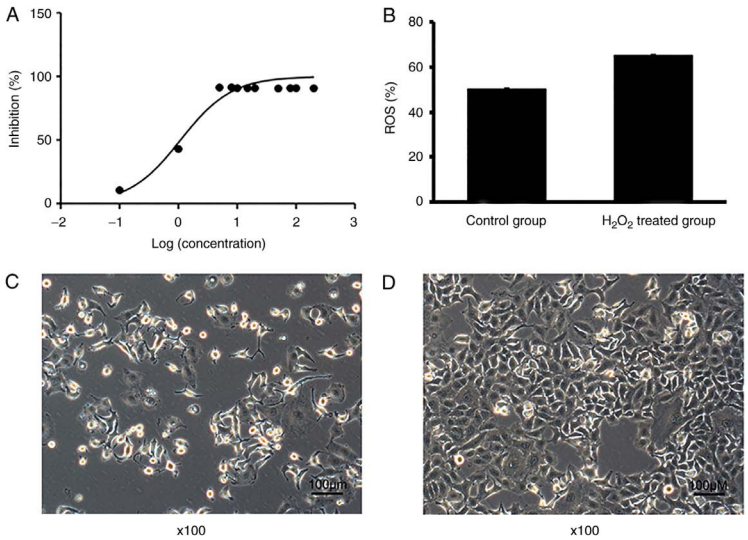

Figure 1. Inhibitory effect of H_2O_2 on the proliferation of A549 cells. (A) MTT dose response curve of the inhibitory effect of H_2O_2 on A549 cells. The best-fit values were: logIC_{50}, 0.037 (570 nm); HillSlope, 0.99; IC_{50}, 1.09 (570 nm). (B) ROS production in H_2O_2-treated A549 cells analysed via the Fluorometric method. Images of (C) H_2O_2-treated and (D) untreated (control) A549 cells. ROS, reactive oxygen species; H_2O_2, hydrogen peroxide; IC_{50}, half maximal inhibitory concentration.

system (Applied Biosystems; Thermo Fisher Scientific, Inc.). The primer sequences are listed in Table I. The following thermocycling conditions were applied: 95˚C for 30 sec, followed by 40 cycles at 95˚C for 5 sec, 60˚C for 15 sec and 72˚C for 10 sec and 72˚C for 7 min for final extension. Data were presented as a relative average value ± SEM after normalization with the average value of the housekeeping gene GAPDH. Direct comparison was performed between the control and H_2O_2-treated groups for the same gene and $2^{-\Delta\Delta Cq}$ method was used for the relative quantification of gene expression (16).

Functional enrichment analysis of DEGs. Gene Ontology (GO) analysis, which organises genes into hierarchical categories and identifies the gene regulatory network based on biological processes (BP), molecular functions (MF) and cellular components (CC), was used for the genes and gene products. Additionally, Kyoto Encyclopedia of Genes and Genomes (KEGG) pathway analysis was used to identify significant pathways of the genes and enriched gene products. The Database for Annotation, Visualization and Integrated Discovery (DAVID; https:/david.ncifcrf.gov/) was used for GO and KEGG functional annotation of genes with P<0.05.

Analysis of the bisulphite sequencing data. Flexbar version 3.0 software (https://github.com/seqan/flexbar) was used to guarantee the high quality of the sequence reads in three steps: In step 1, the low-quality base calls were trimmed, step 2 removed the adaptor and step 3 filtered the PCR duplication. The absolute methylation level was measured by the enrichment of CpG fractions in the genome after treatment with sodium bisulfite. The microarray reads were aligned to the reference sequence and the methylation called base-by-base in the reads with a coverage >10 using the software BSMAP (whole genome bisulphite sequence MAPing program, http://code.google.com/p/bsmap/) Subsequently, the proportion of cytosine and thymine bases was calculated at CG positions among the bisulphite sequencing reads aligned to the reference sequence as the methylation level. The DMRs were identified using the methylKit R package (from R version 3.6.3).

Association analysis between gene expression levels and DNA methylation. Genes with significant changes in expression (P<0.05) were categorised into four groups based on their changes in gene expression (E) and methylation levels (M): Group 1 corresponds to high methylation and upregulated genes (log2 fold change >0.5; E^+ and M^+); Group 2 to high methylation and downregulated genes (log2 fold change <1.5; E^- and M^+); Group 3 to low methylation and upregulated genes (log2 fold change >1.5; E^+ and M^-); and Group 4 to low methylation and downregulated genes (log2 fold change ≤1.5; E^- and M^-). Gene Expression Profiling Interactive Analysis (GEPIA; http://gepia.cancer-pku.cn) was used to analyse the expression levels and the effects of genes on survival with methylation level changes in patients with lung adenocarcinoma (LUAD). GEPIA is a newly developed interactive web server for analysing the RNA sequencing expression data of 9,736 tumours and 8,587 normal samples from The Cancer Genome Atlas and the Genotype-Tissue Expression projects, using a standard processing pipeline.

Statistical analysis. GraphPad Prism (version 5; GraphPad Software, Inc.) was used for statistical analysis. Data are expressed as the mean ± standard error of the mean (SEM). The mean was obtained from three repeats. Differences between two groups were analysed using unpaired Student's t-tests, whereas ≥3 groups were analysed via one-way ANOVA followed by Tukey's post hoc test. In the Kaplan-Meier analysis log-rank test was conducted to assess the survival, or Cramer-von Mises when crossover occurred. All tests performed were two-sided. P<0.05 was considered to indicate a statistically significant difference.

Results

Inhibitory effects of H_2O_2 on the proliferation of A549 cells. The inhibitory effect of H_2O_2 on the proliferation of A549 cells was concentration-dependent (Fig. 1A), with an IC_{50} of 1.09 mg/l. In addition, the ROS production of A549 cells was markedly increased compared with that of the control group (Fig. 1B). The original images of H_2O_2-treated and

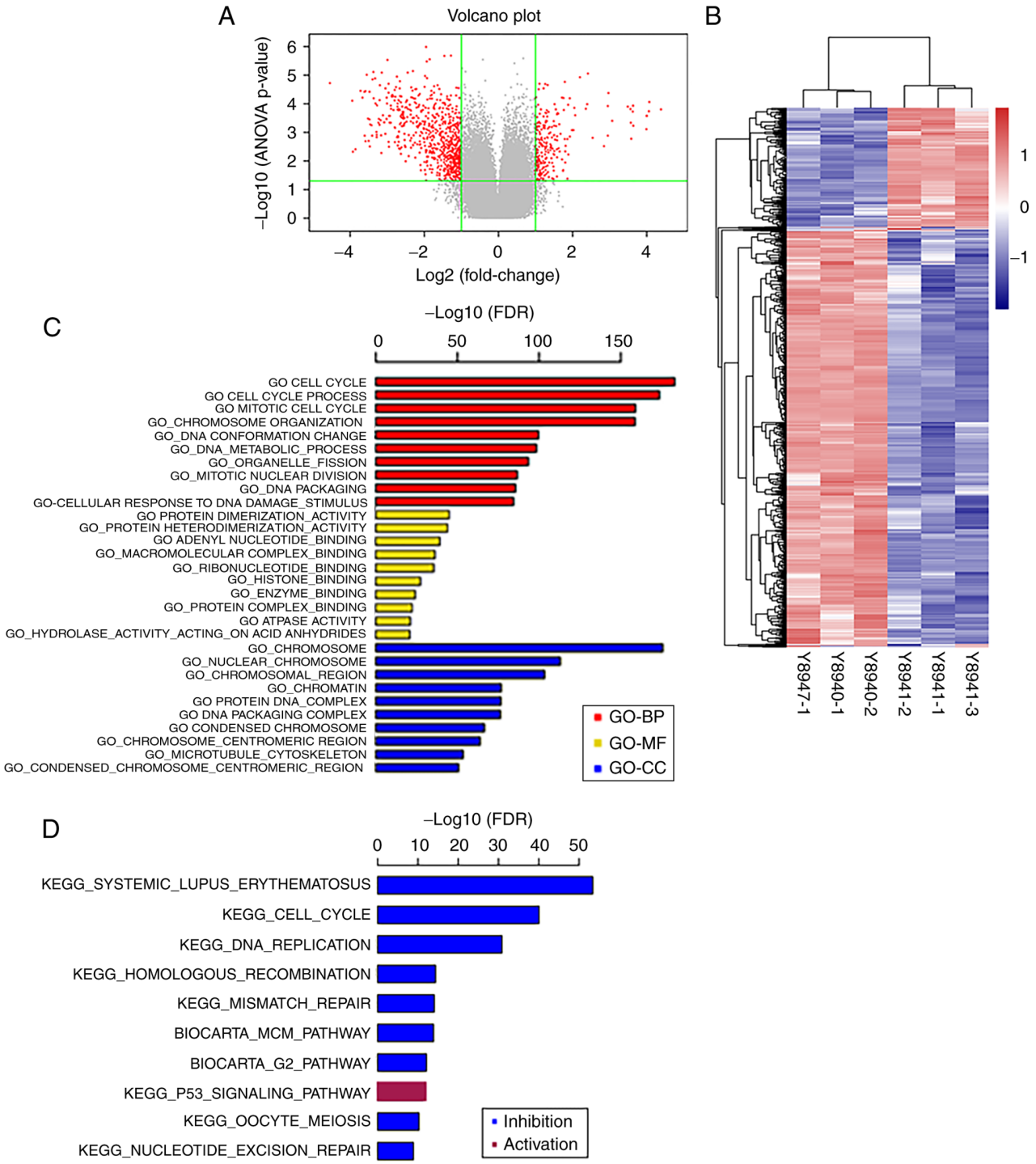

Figure 2. mRNA expression profile. (A) Volcano plot of DEGs. Right red dots indicated upregulated DEGs and left red dots indicated downregulated DEGs. Grey dots were for the genes with expression unchanged. (B) Heatmap of hierarchical clustering for DEGs. Red scale represented upregulated DEGs and blue scale was for downregulated DEGs. (C) GO analysis and (D) KEGG pathway analysis of the DEGs. DEGs, differentially expressed genes; GO, Gene Ontology; KEGG, Kyoto Encyclopedia of Genes and Genomes; BP, biological processes; MF, molecular functions; CC, cellular components; FDR, false discovery rate.

untreated A549 cells were captured using a light microscope (Fig. 1C and D) further confirmed that H_2O_2 inhibited the proliferation of A549 cells.

Analysis of the mRNA expression profiles. A total of 1,026 DEGs, 261 upregulated and 765 downregulated, were identified in H_2O_2-treated A549 cells compared with the control group (Fig. 2A). The heatmap of hierarchical clustering of the DEGs is shown in Fig. 2B. There were 261 upregulated and 766 downregulated genes between H_2O_2-treated A549 cells and the control group. The online analysis tool DAVID was used to identify statistically significant enriched GO terms for the DEGs between the H_2O_2-treated and control groups (Fig. 2C), indicating that the DEGs were mainly enriched in BP, such as 'cell cycle', 'cell cycle process' and 'mitotic cell cycle'. Regarding CC, they were enriched in 'chromosome',

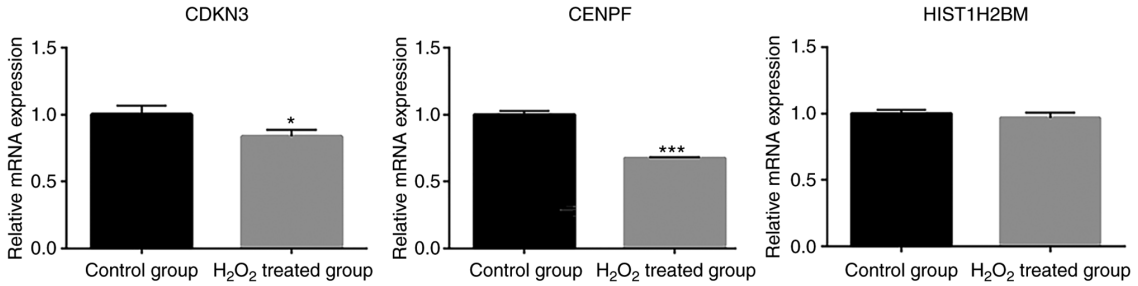

Figure 3. Validation of the expression levels of differentially expressed genes via quantitative PCR. The expression levels of CDKN3 and CENPF were significantly downregulated in H_2O_2-treated A549 cells compared with those in untreated A549 cells (control). HIST1H2BM expression did not differ between the two groups. *P<0.05 and ***P<0.001 vs. Control group. CDKN3, cyclin-dependent kinase inhibitor 3; CENPF, centromere protein F; HIST1H2BM, histone cluster 1 H2B family member M; H_2O_2, hydrogen peroxide.

'nuclear chromosome' and 'chromosomal region'. In addition, MF analysis revealed that the genes were enriched in 'protein dimerization activity', 'protein heterodimerization activity', 'adenyl nucleotide binding' and 'macromolecular complex binding'. KEGG analysis revealed that the DEGs were enriched in 'systemic lupus erythematosus', 'cell cycle', 'DNA replication' and 'homologous recombination' (Fig. 2D). qPCR was used to verify the expression levels of DEGs in A549 cells (Fig. 3). Association analysis of the gene expression and methylation levels revealed that several genes were downregulated and hypermethylated, including cyclin-dependent kinase inhibitor 3, denticleless E3 ubiquitin protein ligase homolog, centromere protein (CENP)F, kinesin family member (KIF)20A, CENPA, KIF11, PCNA clamp associated factor (PAF) and GINS complex subunit 2. Therefore, these genes were chosen to be verified by qPCR. Consistent with the gene expression microarray, the expression levels of cyclin-dependent kinase inhibitor 3 (CDKN3; NCBI_1033) and centromere protein (CENP)F (NCBI_1063) were significantly downregulated in H_2O_2-treated A549 cells compared with those in untreated cells (Fig. 3). The expression levels of H2B clustered histone 14 (H2BC14 NCBI_8342) were decreased slightly in H_2O_2-treated A549 cells, which was also consistent with the microarray results.

Analysis of the DNA methylation expression profiles. RRBS was used to annotate differentially methylated sites between H_2O_2-treated A549 cells and the control group. The CpGs were grouped based on the genomic position, with a similar distribution of CpGs in both groups (Fig. 4A). Additionally, the average methylation level was calculated, with a similar distribution in both groups (Fig. 4B). In total, 29,755 differentially methylated CpG sites were identified; 15,365 of them were more methylated and 14,390 were less methylated in the A549 cells treated with H_2O_2 compared with in the untreated cells. Among the differentially methylated CpG sites, the top 20 were annotated (Table II). The differences in methylation levels in the same region between two samples was calculated to identify the DMRs. The top 10 DMRs were annotated (Table III), suggesting that there was a difference in the methylation levels between the two groups. In addition, the analysis at the region level revealed that 1,575 DMRs occurred in the gene promoters. GO analysis revealed that the genes were enriched in the terms 'extracellular space', 'extracellular matrix', 'neuron protein' and 'perikaryon' (Table IV). KEGG pathway analysis

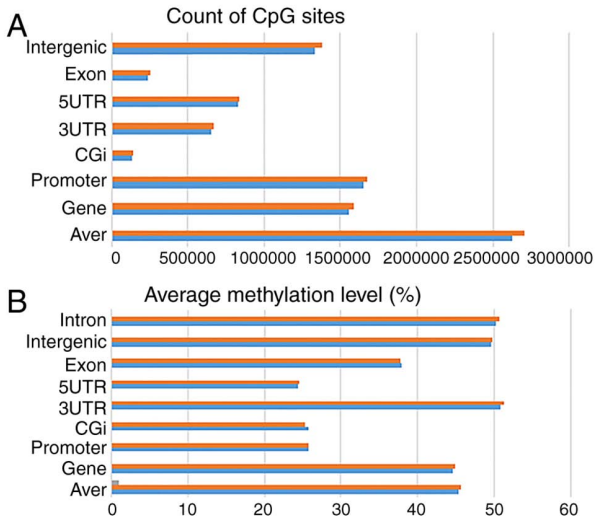

Figure 4. Distribution of CpG sites and the average methylation level in the genome. Distribution of (A) CpG sites and (B) the average methylation level in the genome for the H_2O_2-treated group (orange columns) and untreated (control) group (blue columns). Grey lines in the 'Aver' represented the same CpG counts or the same methylation level. UTR, untranslated region; Aver, average.

revealed that the genes were enriched in 'hsa04723: Retrograde endocannabinoid signalling', 'hsa05032: morphine addiction' and 'hsa04726: Serotonergic synapse' (Table V).

Association analysis of gene expression and methylation levels. The association analysis indicated that genes with a high methylation difference always resulted in a difference in the gene expression levels. Regarding hypermethylation located in the gene body, the top genes that showed greatest difference in methylation between groups included H2BC14 (NCBI_8342), CDKN3 (NCBI_1033), denticleless E3 ubiquitin protein ligase homolog (DTL; NCBI_51514) and CENPF (NCBI_1063) (data not shown). Consistent with the present results, all genes except H2BC14 were upregulated in LUAD tumour tissues compared with normal tissues when analysing the gene expression profiling data using the online tool GEPIA (Fig. 5A). Furthermore, the gene expression levels increased with increasing stages of LUAD (Fig. 5B), and low expression levels were associated with improved survival compared with high expression levels (Fig. 5C). Regarding the hypermethylation in the promoter of genes, the top genes

Table II. Top 20 hypermethylated and top 20 hypomethylated CpG sites between the H_2O_2-treated and control groups.

Chromosome	Position	Strand	P-value	q value	meth.diff (%)	Gene	Gene type	Function element
chr17	78452227	-	$2.56x10^{-24}$	$1.99x10^{-20}$	83.53	NA	NA	Intergenic
chr9	140951580	-	$1.95x10^{-21}$	$6.20x10^{-18}$	81.25	CACNA1B	Protein_coding	Gene
chr11	973547	+	$8.04x10^{-28}$	$1.89x10^{-23}$	79.07	AP2A2	Protein_coding	Gene
chr1	241588198	-	$7.38x10^{-19}$	$1.04x10^{-15}$	78.81	RP11-527D7.1	lincRNA	Gene
chr6	26210354	+	$1.60x10^{-29}$	$7.75x10^{-25}$	77.46	NA	NA	Intergenic
chr15	44068996	+	$9.65x10^{-15}$	$3.34x10^{-12}$	76.54	RP11-296A16.1	Protein_coding	Gene
chr11	19893199	+	$1.90x10^{-17}$	$1.70x10^{-14}$	76.37	NAV2	Protein_coding	Gene
chr16	65732093	+	$5.75x10^{-14}$	$1.50x10^{-11}$	76.28	NA	NA	Intergenic
chr8	95654198	+	$1.25x10^{-21}$	$4.43x10^{-18}$	75.61	ESRP1	Protein_coding	Gene
chrX	133119214	+	$3.80x10^{-18}$	$4.25x10^{-15}$	74.86	GPC3	Protein_coding	Gene
chrX	153734771	+	$2.39x10^{-29}$	$1.04x10^{-24}$	73.91	FAM3A	Protein_coding	Gene
chr7	157697656	+	$7.23x10^{-25}$	$6.57x10^{-21}$	73.88	PTPRN2	Protein_coding	Gene
chr11	64659131	-	$5.57x10^{-22}$	$2.16x10^{-18}$	73.82	MIR194-2	lincRNA	Gene
chr4	131947017	-	$9.96x10^{-17}$	$6.84x10^{-14}$	NA	NA	NA	Intergenic
chr17	78452271	-	$3.26x10^{-19}$	$5.17x10^{-16}$	73.02	NA	NA	Intergenic
chr20	61983851	-	$7.26x10^{-15}$	$2.61x10^{-12}$	72.55	CHRNA4	Protein_coding	Gene
chr2	467136	-	$2.11x10^{-18}$	$2.56x10^{-15}$	72.25	NA	NA	Intergenic
chr7	426119	+	$2.46x10^{-12}$	$3.61x10^{-10}$	71.92	NA	NA	Intergenic
chr8	8632457	-	$2.46x10^{-25}$	$2.50x10^{-21}$	71.11	RP11-211C9.1	lincRNA	Gene
chr15	44069009	+	$4.02x10^{-12}$	$5.46x10^{-10}$	70.47	RP11-296A16.1	Protein_coding	Gene
chr16	34622413	+	$8.19x10^{-20}$	$1.57x10^{-16}$	-87.5	RP11-488I20.3	lincRNA	Gene
chr3	32858837	+	$3.20x10^{-28}$	$8.63x10^{-24}$	-83.04	TRIM71	Protein_coding	Promoter
chr16	34622419	+	$2.00x10^{-17}$	$1.77x10^{-14}$	-81.25	RP11-488I20.3	lincRNA	Gene
chr9	136150995	+	$1.11x10^{-15}$	$5.36x10^{-13}$	-81.09	ABO	Processed_transcript	Promoter
chr15	62110720	-	$1.23x10^{-21}$	$4.39x10^{-18}$	-80.31	NA	NA	Intergenic
chr3	38071105	+	$3.97x10^{-30}$	$2.34x10^{-25}$	-80.22	PLCD1	Protein_coding	Gene
chr19	1323858	-	$5.41x10^{-28}$	$1.34x10^{-23}$	-79.82	MUM1	Protein_coding	Gene
chr15	79092872	-	$3.36x10^{-16}$	$1.94x10^{-13}$	-78.5	ADAMTS7	Protein_coding	Gene
chr19	47979937	-	$9.68x10^{-21}$	$2.47x10^{-17}$	-76.98	KPTN	Protein_coding	Gene
chr19	39342337	-	$3.42x10^{-22}$	$1.41x10^{-18}$	-76.4	HNRNPL	Protein_coding	Gene
chr5	179228528	-	$1.87x10^{-20}$	$4.36x10^{-17}$	-75.95	MGAT4B	Protein_coding	Gene
chr1	216275907	+	$1.71x10^{-18}$	$2.16x10^{-15}$	-75.06	USH2A	Protein_coding	Gene
chr3	109051010	-	$1.61x10^{-18}$	$2.05x10^{-15}$	-74.89	DPPA4	Protein_coding	Gene
chr4	81111777	+	$1.42x10^{-19}$	$2.50x10^{-16}$	-73.33	PRDM8	Protein_coding	Gene
chr3	13816124	+	$1.33x10^{-18}$	$1.73x10^{-15}$	-72.31	NA	NA	Intergenic
chr10	79470698	-	$1.63x10^{-20}$	$3.87x10^{-17}$	-72.08	NA	NA	Intergenic
chr14	104940386	+	$4.22x10^{-19}$	$6.40x10^{-16}$	-71.71	NA	NA	Intergenic
chr10	123389019	+	$4.70x10^{-16}$	$2.57x10^{-13}$	-71.57	NA	NA	Intergenic
chr16	60247513	-	$1.19x10^{-14}$	$3.98x10^{-12}$	-71.48	NA	NA	Intergenic
chr1	53098973	+	$2.36x10^{-15}$	$1.01x10^{-12}$	-70.82	FAM159A	Protein_coding	Promoter

meth.diff, methylation difference; NA, not available.

showing the most notable difference in methylation included kinesin family member (KIF)20A (NCBI_10112), CENPA (NCBI_1058), KIF11 (NCBI_3832), PCNA clamp-associated factor (PAF, NCBI_9768) and GINS complex subunit 2 (GINS2; NCBI_51659) (data not shown), which exhibited the same trends as aforementioned in LUAD (Fig. 6). The findings showed that genes that were downregulated in H_2O_2-treated cells were more highly expressed in tumour samples with poor prognosis. The biological function of these genes requires further study.

Although the gene expression and methylation levels were in accordance, there were some differences between the H_2O_2-treated and the control group (Fig. 7A and B). Integrated analysis revealed that the total expression levels of the genes

Table III. Top 10 hypermethylated and top 10 hypomethylated CpG regions between the H_2O_2-treated and control groups.

Chromosome	Start	End	P-value	meth.diff (%)	Gene	Gene type	Function element
chr10	3558001	3559000	$3.29x10^{-51}$	74.40	NA	NA	Intergenic
chr4	110000000	110000000	$8.88x10^{-27}$	70.70	CCDC109B	Protein_coding	Gene
chr16	68293001	68294000	$6.80x10^{-24}$	68.70	PLA2G15	Protein_coding	Gene
chr15	85383001	85384000	$5.03x10^{-21}$	67.80	ALPK3	Protein_coding	Gene
chr17	7696001	7697000	$1.36x10^{-26}$	66.90	DNAH2	Protein_coding	Gene
chr5	10620001	10621000	$9.08x10^{-36}$	65.00	ANKRD33B	Protein_coding	Gene
chr5	68631001	68632000	$3.05x10^{-27}$	64.20	CCDC125	Protein_coding	Promoter
chr19	13025001	13026000	$9.50x10^{-19}$	63.50	GCDH	Protein_coding	Gene
chr20	62044001	62045000	$6.57x10^{-28}$	61.20	KCNQ2	Protein_coding	Gene
chr11	6705001	6706000	$1.19x10^{-89}$	60.10	MRPL17	Protein_coding	Promoter
chr17	1112001	1113000	$1.15x10^{-20}$	-72.40		Protein_coding	Gene
chr9	126000000	126000000	$4.44x10^{-18}$	-69.00	DENND1A	Protein_coding	Gene
chr15	86220001	86221000	$4.86x10^{-17}$	-65.60	AKAP13	Protein_coding	Gene
chr11	66061001	66062000	$7.37x10^{-35}$	-65.20	TMEM151A	Protein_coding	Gene
chr15	72412001	72413000	$1.35x10^{-20}$	-65.10	SENP8	Protein_coding	Gene
chr1	67323001	67324000	$5.58x10^{-22}$	-64.70	WDR78	Protein_coding	Gene
chr22	37572001	37573000	$2.11x10^{-17}$	-64.10	RP1-151B14.6	Antisense	Gene
chr7	105000000	105000000	$2.25x10^{-23}$	-63.80	RINT1	Protein_coding	Gene
chr16	65731001	65732000	$1.97x10^{-17}$	-62.50	NA	NA	Intergenic
chr20	50471001	50472000	$3.02x10^{-16}$	-61.70	RP5-1112F19.2	lincRNA	Gene

meth.diff, methylation difference; NA, not available.

decreased as the methylation levels increased. Upstream of genes, the high methylation levels decreased gene expression levels compared with low methylation levels (Fig. 7C). Furthermore, the methylation and gene expression levels in both study groups were associated. Consistent with a previous report (9), most genes with low expression levels had high methylation levels (Fig. 7D).

Discussion

In the present study, genome-wide analyses of mRNA expression and DNA methylation profiles were employed to explore the inhibitory mechanism of H_2O_2 on the proliferation of A549 lung cancer cells. Several genes, including CDKN3, DTL, CENPF, KIF20A, CENPA, KIF11, PAF and GINS2, were downregulated and hypermethylated in H_2O_2-treated A549 cells compared with in untreated cells, suggesting that they may have important roles in the inhibitory process of H_2O_2 on the proliferation of A549 cells.

Increasing evidence has revealed that gene expression can be affected by epigenetic regulatory mechanisms, with DNA methylation at CpG islands occurring around the genomic promoter regions (17,18). Hypermethylation can repress transcription and downregulate gene expression by altering the chromatin framework, thereby leading to cancer initiation and progression (19). Consistent with a previous report (19), the present study identified several genes associated with the progression of lung cancer that were downregulated and hypermethylated in the gene bodies in H_2O_2-treated cells, including CDKN3, DTL and CENPF. The expression levels of these genes increased with the progression of LUAD, and low expression levels were associated with an improved survival, further proving their critical roles in the pathological processes of lung cancer. Although the expression levels of HIST1H2BM were not significantly different between LUAD and normal control samples, this gene was identified as a candidate epigenetic biomarker in LUAD through genome-wide analysis comparing the methylation patterns (20). Another study obtained similar results, revealing that increased expression levels of HIST1H2BM were associated with a poor survival in patients with LUAD and may act as a potential biomarker of drug synergy for the future clinical trials (21). Although in the previous study CDK3 has been reported as a tumour suppressor by maintaining the proper number of centrosomes (22), CDKN3 has also been demonstrated to be a potential poor prognostic marker in LUAD through the systematic analysis of datasets in Lung Cancer Explorer (23). Another report further proved that CDKN3 upregulation, which is mainly caused by the increase of mitotic activity, may be associated with poor survival in patients with LUAD, arguing against CDKN3 as a tumour suppressor (24).

In the present study, genes including KIF20A, CENPA, KIF11, PAF and GINS2, were downregulated in H_2O_2-treated cells and hypermethylated in the gene promoters. While these genes were also upregulated in LUAD tumour samples and their expression levels increased with the progression of LUAD, suggesting that they may have crucial roles in the development of tumours. Accumulating evidence has identified

Table IV. GO analysis of the genes with differentially methylated regions in the promoter of genes.

Category	Term	Count	Genes
GOTERM_CC_DIRECT	GO:0005615~extracellular space	88	GDF3, PXDN, NOG, SLURP1, LYPD3, IL16, KIAA0556, GDF6, LTBP4, EDN2, CRHBP, TNFSF14, TNFSF13, DLK1, MCF2L, MMRN2, SCT, GPC5, AZGP1, APOE, CETP, CFD, ACTN4, IL27, ZNF649, C10ORF99, CST1, MFGE8, CBR3, SSPO, CTSV, PROC, RETN, CBLN4, AMH, CHGA, THBD, GNB2, SERPINF1, F3, SERPINB8, CPXM1, ULBP2, NPPC, C1QL4, UBB, WNT9A, ADAMTS5, TF, RBP4, MFNG, PODN, PRTN3, NDP, CLU, DSCAML1, PF4, CXCL6, NRN1, CCL5, CHIT1, ADCYAP1, CPZ, AGT, LEFTY2, TFF2, VWC2L, ENTPD6, HGFAC, OLFM1, BMP4, FLRT3, BGLAP, PRSS57, HSPG2, TNFSF9, FRZB, KRT35, CLEC11A, MUC4, NBL1, TSLP, DKK3, PPIA, KRT78, LIPG, NRN1L, METRNL
GOTERM_CC_DIRECT	GO:0031012~extracellular matrix	26	FGFR2, HIST1H4L, PXDN, PRTN3, LTBP4, NDP, ADAMTSL5, CLU, HSPG2, MMP17, MFGE8, EMILIN3, NDNF, COL5A1, RPS3, MMRN2, LAMA2, SERPINF1, APOE, F3, LEFTY2, HIST1H4E, ADAMTS10, TGFB1I1, B4GALT7, HSPA9
GOTERM_CC_DIRECT	GO:0043005~neuron projection	22	GDI1, ACTN4, SLC6A12, ADCYAP1R1, SLC6A4, WRN, ATP13A2, SHANK2, CTSV, SHANK3, TRPM2, SLC32A1, ATP2B4, P2RX1, HDAC1, ARPC2, BCL11B, CHRNB4, ABAT, CYGB, NSMF, UBB
GOTERM_CC_DIRECT	GO:0043204~perikaryon	12	SLC8A3, MAPK1, BGLAP, CRHBP, EFNA2, CNTNAP2, NSMF, NTSR1, CTSV, OLFM1, TRPM2, NEURL1
GOTERM_CC_DIRECT	GO:0048471~perinuclear region of cytoplasm	41	SLC8A3, NANOS3, TF, MAL2, HIP1R, ABCD1, SLC39A13, SLC39A12, CLU, TRAPPC2L, CABP7, PLVAP, NXT2, SLK, NMRAL1, ARHGAP1, MMD2, NDRG2, EHD2, C9ORF24, CCAR1, DLG1, ACTN4, LDB3, CIDEB, ACKR3, TPD52L2, KAT5, PRKCD, MT1X, CHGA, SERPINF1, HDAC1, GNB2, VAMP8, TPPP, ATP9A, CDK2AP1, MEX3D, ABL1, NEURL1

GO, Gene Ontology.

that KIF20A is a major gene associated with various types of cancer, such as pancreatic cancer (25), gastric cancer (26) and glioma (27). Ni *et al* (28) identified KIF20A as a potential prognostic biomarker that was associated with the pathogenesis of NSCLC through a series of bioinformatics methods. Gasnereau *et al* (29) further proved that the expression levels of KIF20A increased during the proliferation of hepatocytes and the occurrence of lung cancer.

Epigenetic mechanisms, such as DNA methylation, are essential for the regulation of gene expression, and aberrant epigenetic alterations can lead to pathological conditions, including cancer (30). DNA methylation close to the promoters of a gene has been reported to repress gene expression (31), whereas the effect of methylation in the gene body is unclear. Xie *et al* (31) demonstrated that ROS downregulated the expression levels of the AT-rich interaction domain 1A via methylation of its promoter during the pathogenesis of endometriosis, whereas Wang *et al* (32) revealed that methylation in the inositol-triphosphate 3-kinase A gene body regulated gene expression and may serve as an early diagnostic marker

Table V. KEGG pathway analysis of the genes with differentially methylated regions in the promoter of genes.

KEGG pathway	Count	P-value	Genes
hsa04723:Retrograde endocannabinoid signaling	13	7.62×10^{-4}	GABRD, GABRG2, GABRG3, CACNA1S, KCNJ3, GRM1, SLC32A1, GNG8, GNGT1, MAPK1, GNB2, FAAH, GNG4
hsa05032:Morphine addiction	12	≤0.001	GNG8, GABRD, SLC32A1, GNGT1, GABRG2, GABRG3, GNB2, PDE1C, GRK4, PDE4D, GNG4, KCNJ3
hsa04726:Serotonergic synapse	13	≤0.001	MAOA, SLC6A4, RAF1, CACNA1S, KCNJ3, GNG8, MAPK1, GNGT1, ALOX15, HTR1B, GNB2, GNG4, HTR2A
hsa04724:Glutamatergic synapse	13	≤0.001	GRIK1, GRM1, KCNJ3, SHANK2, SHANK3, GNG8, GRM4, MAPK1, GNGT1, GNB2, PPP3CC, GNG4, SLC1A1
hsa04727:GABAergic synapse	10	≤0.001	GNG8, GABRD, SLC32A1, GNGT1, GABRG2, GABRG3, GNB2, ABAT, GNG4, CACNA1S
hsa05020:Prion diseases	5	≤0.001	C1QA, MAPK1, NCAM2, C1QB, CCL5

KEGG, Kyoto Encyclopedia of Genes and Genomes.

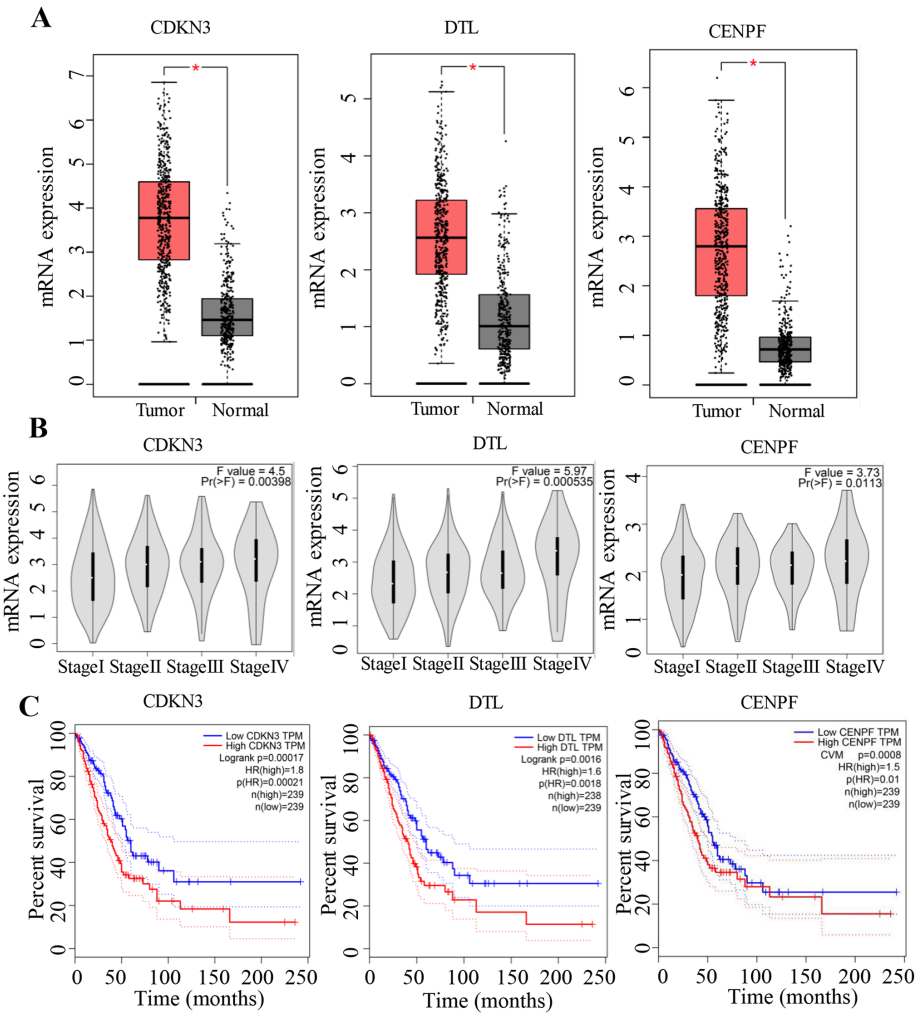

Figure 5. Validation of the expression levels of genes in which hypermethylation occurred in the gene body, with the RNA sequencing expression data of LUAD (from GEPIA). (A) Gene expression levels in 483 LUAD samples and 347 normal control samples. (B) Gene expression levels at different stages of LUAD (From GEPIA). (C) Overall survival curves based on high and low gene expression levels. *P<0.05. LUAD, lung adenocarcinoma; CDKN3, cyclin-dependent kinase inhibitor 3; CENPF, centromere protein F; DTL, denticleless E3 ubiquitin protein ligase homolog; HR, hazard ratio; TPM, transcript per million.

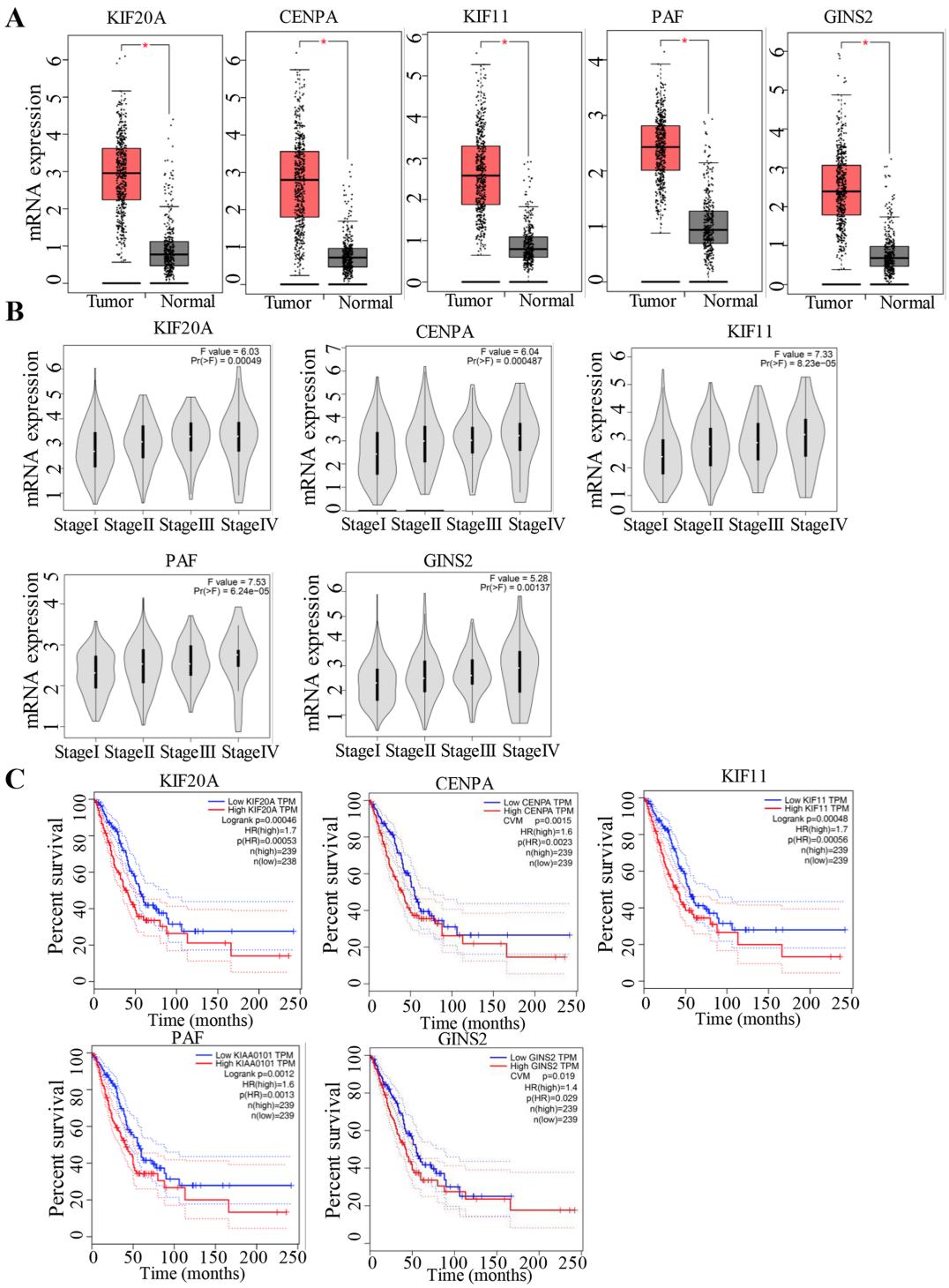

Figure 6. Validation of the expression levels of genes in which hypermethylation occurred in the gene promoter, with the RNA sequencing expression data of LUAD (from GEPIA). (A) Gene expression levels in 483 LUAD samples and 347 normal control samples. (B) Gene expression levels at different stages of LUAD. (C) Overall survival curves based on low and high gene expression levels. *P<0.05. LUAD, lung adenocarcinoma; KIF20A/11, kinesin family member 20A/11; CENPA, centromere protein A; GINS2, GINS complex subunit 2; PAF, PCNA clamp-associated factor; HR, hazard ration; TPM, transcript per million.

in lung cancer. The results of the present study revealed that in the upstream region of genes, high methylation levels were associated with decreased gene expression compared with a low methylation level, whereas in the gene body or downstream of genes, the methylation level did not markedly affect gene expression. Therefore, it was hypothesized that DNA methylation in the upstream region of genes, particularly near the promoter, may have different mechanisms than in the gene body region. Future research is required to increase the understanding of the mechanisms and critical roles of different methylation regions in various cellular processes.

The present study identified several genes that were downregulated and hypermethylated in A549 cells treated with H_2O_2, suggesting that they may have vital roles in H_2O_2-induced

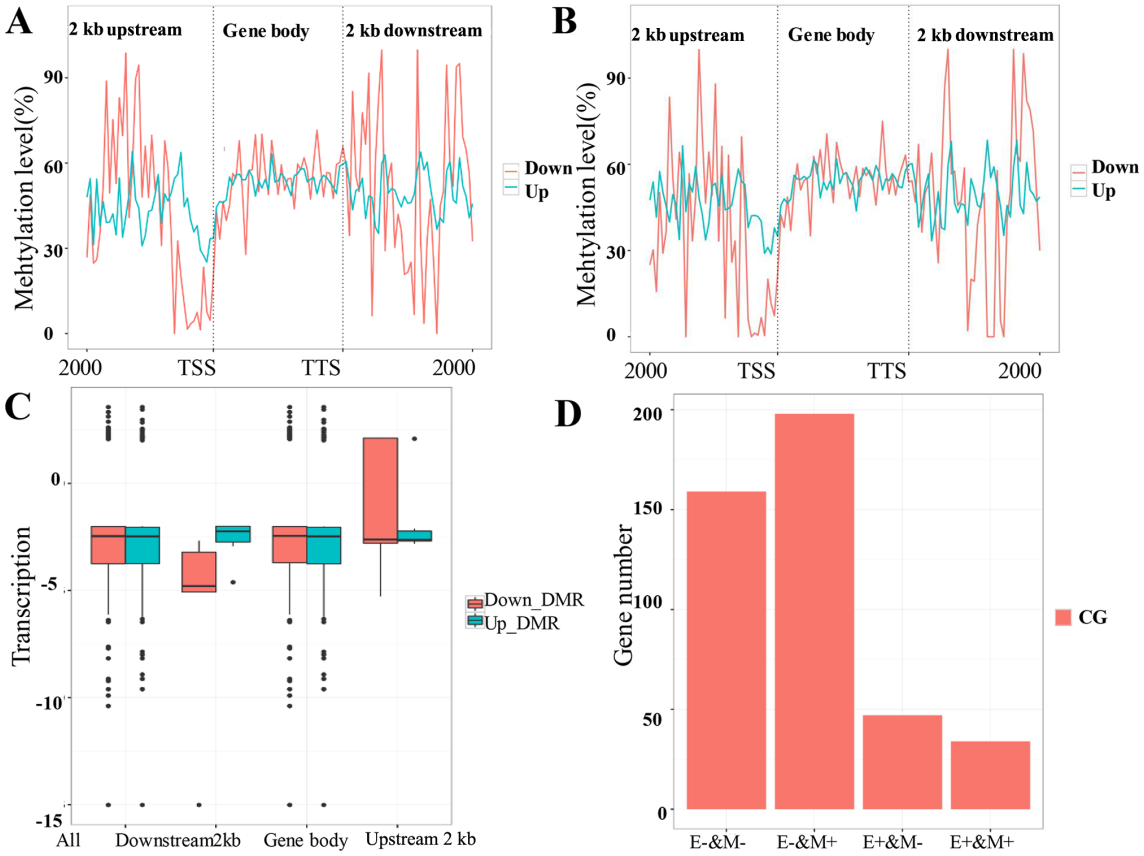

Figure 7. Association analysis of gene expression and methylation levels. Gene expression and methylation levels in (A) the control group and (B) the hydrogen peroxide-treated group. (C) Gene expression levels of DMRs around the gene position. Gene expression was presented as median and interquartile range. (D) Genes in both study groups with different expression and methylation levels. All, all the DMRs; Downstream 2 kb, DMRs located in promoter downstream 2 kb; Gene body, DMRs located in gene's body; Upstream 2 kb, DMRs located in promoter upstream 2 kb; E+, high expression; E-, low expression; M+, high methylation; M-, low methylation; DMR, differentially methylated region; NC, negative control.

inhibition of the proliferation of A549 cells. However, further experiments are required to validate the specific function of these genes in A549 cells. In addition, the association analysis between gene expression and methylation levels indicated that their association may be far more complicated than previously thought, with the effects of DNA methylation on gene expression appearing to be position-dependent; whether the effects are also sequence-dependent requires further investigation. In conclusion, the present study integrated mRNA expression and DNA methylation profiling, providing novel insights into the molecular mechanisms underlying the pathological processes of lung cancer, and contributed to the identification of biomarkers and novel strategies for drug design for the treatment of lung cancer.

Acknowledgements

Not applicable.

Funding

The present work was supported by grants from the Affiliated Hospital of Youjiang Medical University for Nationalities Outstanding Scholar Funding (grant no. R20196313) and Doctorate Awarding Unit Funding of the Affiliated Hospital of Youjiang Medical University for Nationalities [grant no. (2019)48]. The funders had no role in the design of the study, the collection, analyses or interpretation of data, the writing of the manuscript or the decision to publish the results.

Availability of data and materials

The datasets generated and/or analysed during the current study are available from the corresponding author on reasonable request.

Authors' contributions

YL was involved in the design of the study, analysis and interpretation of data, and drafting the manuscript. BY gave final approval of the version of the manuscript to be published and was involved in data analysis. SH revised the manuscript critically for important intellectual content, and was involved in the acquisition and analysis of data. ZW made substantial contributions to conception and design. All authors have read and approved the final manuscript.

Ethics approval and consent to participate

Not applicable.

Patient consent for publication

Not applicable.

Competing interests

The authors declare that they have no competing interests.

References

1. Collins Y, Chouchani ET, James AM, Menger KE, Cochemé HM and Murphy MP: Mitochondrial redox signalling at a glance. J Cell Sci 125: 801-806, 2012.
2. Forkink M, Basit F, Teixeira J, Swarts HG, Koopman WJH and Willems PHGM: Complex I and complex III inhibition specifically increase cytosolic hydrogen peroxide levels without inducing oxidative stress in HEK293 cells. Redox Biol 6: 607-616, 2015.
3. Zhang YW, Zheng Y, Wang JZ, Lu XX, Wang Z, Chen LB, Guan XX and Tong JD: Integrated analysis of DNA methylation and mRNA expression profiling reveals candidate genes associated with cisplatin resistance in non-small cell lung cancer. Epigenetics 9: 896-909, 2014.
4. Wan M, Bennett BD, Pittman GS, Campbell MR, Reynolds LM, Porter DK, Crowl CL, Wang X, Su D, Englert NA, *et al*: Identification of smoking-associated differentially methylated regions using reduced representation bisulfite sequencing and cell type-specific enhancer activation and gene expression. Environ Health Perspect 126: 047015, 2018.
5. Deng F, Yang ZF and Sun CQ: The role of Notch1 genes in lung cancer A594 cells and the impact on chemosensitivity. Eur Rev Med Pharmacol Sci 21: 2659-2664, 2017.
6. Park W: MAPK inhibitors, particularly the JNK inhibitor, increase cell death effects in H_2O_2-treated lung cancer cells via increased superoxide anion and glutathione depletion. Oncol Rep 39: 860-870, 2018.
7. Sun C, Jin W and Shi H: Oligomeric proanthocyanidins protects A549 cells against H_2O_2-induced oxidative stress via the Nrf2-ARE pathway. Int J Mol Med 39: 1548-1554, 2017.
8. Bird A: DNA methylation patterns and epigenetic memory. Genes Dev 16: 6-21, 2002.
9. Rauscher GH, Kresovich JK, Poulin M, Yan L, Macias V, Mahmoud AM, Al-Alem U, Kajdacsy-Balla A, Wiley EL, Tonetti D and Ehrlich M: Exploring DNA methylation changes in promoter, intragenic, and intergenic regions as early and late events in breast cancer formation. BMC Cancer 15: 816, 2015.
10. Chen X, Liu L, Mims J, Punska EC, Williams KE, Zhao W, Arcaro KF, Tsang AW, Zhou X and Furdui CM: Analysis of DNA methylation and gene expression in radiation-resistant head and neck tumors. Epigenetics 10: 545-561, 2015.
11. Cheah SY, Lawford BR, Young RM, Morris CP and Voisey J: mRNA Expression and DNA methylation analysis of serotonin receptor 2A (HTR2A) in the human schizophrenic brain. Genes (Basel) 8: 14, 2017.
12. Diederich M, Hansmann T, Heinzmann J, Barg-Kues B, Herrmann D, Aldag P, Baulain U, Reinhard R, Kues W, Weissgerber C, *et al*: DNA methylation and mRNA expression profiles in bovine oocytes derived from prepubertal and adult donors. Reproduction 144: 319-330, 2012.
13. Anglim PP, Galler JS, Koss MN, Hagen JA, Turla S, Campan M, Weisenberger DJ, Laird PW, Siegmund KD and Laird-Offringa IA: Identification of a panel of sensitive and specific DNA methylation markers for squamous cell lung cancer. Mol Cancer 7: 62, 2008.
14. Del Real A, Pérez-Campo FM, Fernández AF, Sañudo C, Ibarbia CG, Pérez-Núñez MI, Criekinge WV, Braspenning M, Alonso MA, *et al*: Differential analysis of genome-wide methylation and gene expression in mesenchymal stem cells of patients with fractures and osteoarthritis. Epigenetics 12: 113-122, 2017.
15. Kernaleguen M, Daviaud C, Shen Y, Bonnet E, Renault V, Deleuze JF, Mauger F and Tost J: Whole-genome bisulfite sequencing for the analysis of genome-wide dnamethylation and hydroxymethylation patterns at single-nucleotide resolution. Methods Mol Biol 1767: 311-349, 2018.
16. Riesewijk A, Martín J, van Os R, Horcajadas JA, Polman J, Pellicer A, Mosselman S and Simón C: Gene expression profiling of human endometrial receptivity on days LH+2 versus LH+7 by microarray technology. Mol Hum Reprod 9: 253-264, 2003.
17. Guo K, Elzinga S, Eid S, Figueroa-Romero C, Hinder LM, Pacut C, Feldman EL and Hur J: Genome-wide DNA methylation profiling of human diabetic peripheral neuropathy in subjects with type 2 diabetes mellitus. Epigenetics 14: 766-779, 2019.
18. Navarro A, Yin P, Monsivais D, Lin SM, Du P, Wei JJ and Bulun SE: Genome-Wide DNA methylation indicates silencing of tumor suppressor genes in uterine leiomyoma. PLoS One 7: e33284, 2012.
19. Li P, Shi J, He Q, Hu Q, Wang YY, Zhang LJ, Chan WT and Chen WX: Streptococcus pneumoniae induces autophagy through the Inhibition of the PI3K-I/Akt/mTOR Pathway and ROS Hypergeneration in A549 Cells. PLoS One 10: e0122753, 2015.
20. Daugaard I, Dominguez D, Kjeldsen TE, Kristensen LS, Hager H, Wojdacz TK and Hansen LL: Identification and validation of candidate epigenetic biomarkers in lung adenocarcinoma. Sci Rep 6: 35807, 2016.
21. Ponsuksili S, Trakooljul N, Basavaraj S, Hadlich F, Murani E and Wimmers K: Epigenome-wide skeletal muscle DNA methylation profiles at the background of distinct metabolic types and ryanodine receptor variation in pigs. BMC Genomics 20: 492, 2019.
22. Srinivas V, Kitagawa M, Wong J, Liao PJ and Lee SH: The Tumor suppressor Cdkn3 is required for maintaining the proper number of centrosomes by regulating the centrosomal stability of Mps1. Cell Rep 13: 1569-1577, 2015.
23. Zang X, Chen M, Zhou Y, Xiao G, Xie Y and Wang X: Identifying CDKN3 gene expression as a prognostic biomarker in lung adenocarcinoma via meta-analysis. Cancer Inform 14 (Suppl 2): S183-S191, 2015.
24. Fan C, Chen L, Huang Q, Shen T, Welsh EA, Teer JK, Cai J, Cress WD and Wu J: Overexpression of major CDKN3 transcripts is associated with poor survival in lung adenocarcinoma. Br J Cancer 113: 1735-1743, 2015.
25. Imai K, Hirata S, Irie A, Senju S, Ikuta Y, Yokomine K, Harao M, Inoue M, Tomita Y, Tsunoda T, *et al*: Identification of HLA-A2-restricted CTL epitopes of a novel Tumour-associated antigen, KIF20A, overexpressed in pancreatic cancer. Br J Cancer 104: 300-307, 2011.
26. Yan GR, Zou FY, Dang BL, Zhang Y, Yu G, Liu X and He QY: Genistein-induced mitotic arrest of gastric cancer cells by downregulating KIF20A, a proteomics study. Proteomics 12: 2391-2399, 2012.
27. Saito K, Ohta S, Kawakami Y, Yoshida K and Toda M: Functional analysis of KIF20A, a potential immunotherapeutic target for glioma. J Neurooncol 132: 63-74, 2017.
28. Ni M, Liu X, Wu J, Zhang D, Tian J, Wang T, Liu S, Meng Z, Wang K, Duan X, *et al*: Identification of candidate biomarkers correlated with the pathogenesis and prognosis of non-small cell lung cancer via integrated bioinformatics analysis. Front Genet 9: 469, 2018.
29. Gasnereau I, Boissan M, Margall-Ducos G, Couchy G, Wendum D, Bourgain-Guglielmetti F, Desdouets C, Lacombe ML, Zucman-Rossi J and Sobczak-Thépot J: KIF20A mRNA and its product MKlp2 Are increased during hepatocyte proliferation and hepatocarcinogenesis. Am J Pathol 180: 131-140, 2012.
30. Yang H, Chang F, You C, Cui J, Zhu G, Wang L, Zheng Y, Qi J and Ma H: Whole-genome DNA methylation patterns and complex associations with gene structure and expression during flower development in Arabidopsis. Plant J 81: 268-281, 2014.
31. Xie H, Chen P, Huang HW, Liu LP and Zhao F: Reactive oxygen species downregulate ARID1A expression via its promoter methylation during the pathogenesis of endometriosis. Eur Rev Med Pharmacol Sci 21: 4509-4515, 2017.
32. Wang YW, Ma X, Zhang YA, Wang MJ, Yatabe Y, Lam S, Girard L, Chen JY and Gazdar AF: ITPKA gene body methylation regulates gene expression and serves as an early diagnostic marker in lung and other cancers. J Thorac Oncol 11: 1469-1481, 2016.